4.6 The October 9, 1995 Mexican tsunami.

4.6.1 Introduction

On October 9, 1995, an earthquake of $M_w = 7.9$, centered offshore the states of Jalisco and Colima along the Pacific coast of central Mexico shook the region. This earthquake was the largest event in 60 years along the Northern Middle America Subduction Zone. The fault parameters estimated by the Harvard solution suggest a low-angle thrust mechanism, which can be considered as typical tsunamigenic event for a subduction zone. The displacement caused widespread coastal subsidence, and it was measured by a GPS network installed at Jalisco (Melbourne et. al. 1996). The earthquake caused extensive shaking damage in the vicinity of Manzanillo with many hotels and tall buildings completely destroyed or severely damaged. Approximately 40 people were killed and about 100 injured.

The earthquake set off a tsunami which affected approximately 300*km* of coastline. Tsunami runup ranging from 1 to 5*m* was originally reported in the region from north of Playa de Cuyatlan to south of Tenacatita Bay. In regions with steep onshore topography, the damage was mostly minor, but along the most gentle beaches, the damage was moderate. There was also severe damage in the Port of Manzanillo, where a 12-knot tsunami-induced current caused extreme erosion on the banks of the port. This event provided data on the freefield offshore profile of a tsunami, as the incoming wave was measured by two bottom pressure transducers which had been deployed offshore at 50*m* water depth for a study of internal wave motions; also observations of the height of the leading-depression wave and photographs were taken by eyewitnesses as the wave climbed ashore.

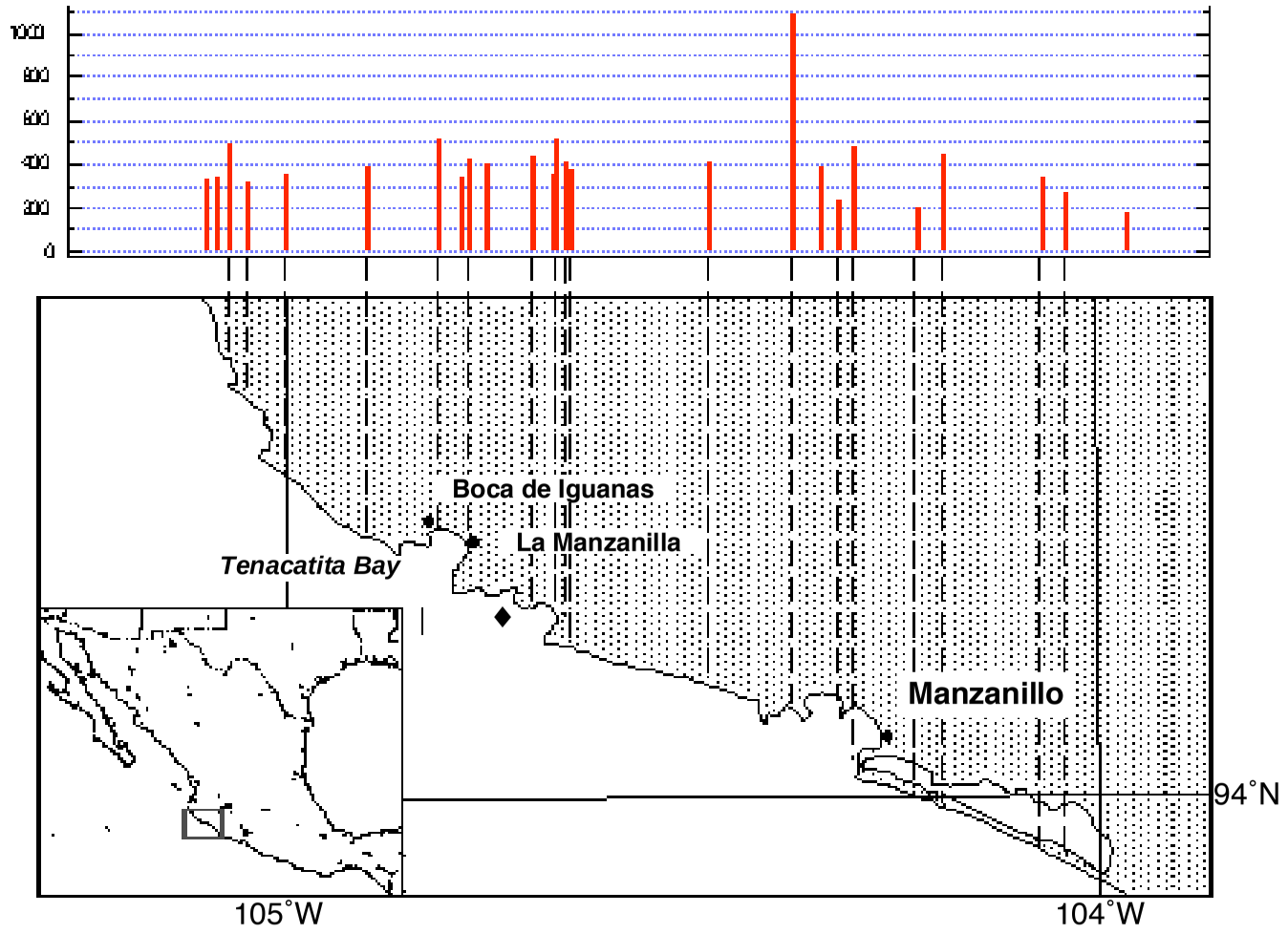

Figure 4.52 The runup measurements along Mexican coast. The epicenter of the earthquake is shown by a star, the location of the pressure transducers is shown by black diamond.

4.6.2 The post-tsunami field survey

The International Tsunami Survey Team from the University of Southern California and from the Centro de Investigacion Cientifica, Desarollo Tecnologico y de Educacion Superior (CICESE) of Ensanada, Mexico, surveyed the area of the tsunami impact. The full report of the survey is published elsewhere (Borrero et al., 1997).

Figure 4.53 The water retreating from the shore of La Manzanilla as the leading depression wave of the tsunami reached the coast.

Figure 4.52 shows measured runup height along the surveyed area of the Mexican coast. Most of the witnesses reported that water receded first and flooded the beaches afterwards, indicating a leading depression wave (Tadepalli and Synolakis, 1994). Near the entrance to Manzanillo harbor, there was extensive damage due to the tsunami currents, which according to local current meters surged up 12 knots. The strong current scoured

away the banks, undermining a road, a local monument and a house, all of which collapsed into the ocean. When the wave began to recede, eyewitnesses reported a whirlpool formed just outside to entrance of the harbor.

On the extreme north end of Santiago Bay is an area of steep cliffs, here the highest runup value of 10.9*m* was measured. Several witnesses reported that the water first withdrew several hundred meters offshore and then rushed in and up the cliff violently splashing over the edge; the cliffs are about 10*m* high with a narrow gravel beach at the bottom.

The most spectacular tsunami damage of this event was observed in the bay of Tenacatita. La Manzanilla is a small town that sits on the southern end of this bay. This small town was completely flooded to a depth of over 2*m* in most areas. The water advanced through the town stopping only when it reached a steep hill 200*m* inland. All eyewitnesses reported a leading-depression wave with the water in the bay retreating several hundred meters, as seen in the photo in Figure 4.53, taken from above La Manzanilla. An eyewitness reported that the "normal" depth at the point of largest withdrawal is 5–6*m*, as he frequently dives for shellfish in the vicinity of the exposed rocks, this report provides perhaps the first definite estimation of a lower limit of the amplitude of the leading depression wave. When the water began to return and advance, it did so like "a fast rising tide". Fortunately, the people on the beach were able to outrun the advancing water and no one was killed. One resident of La Manzanilla was able to take a sequence of photos as the water advanced through his town. (see Figure 4.54). The rest of this sequence and other tsunami survey pho-

tos can be seen on the University of Southern California's Tsunami Web Site at: www.usc.edu/dept/tsunamis/.

Figure 4.54 The tsunami wave inundating streets of La Manzanilla.

On the northern end of Tenacatita Bay, there is a small river inlet and a camping area known as Boca de Iguanas. The land here is quite flat and low. After the initial withdrawal, the water came in with much greater force than in La Manzanilla. The beach-facing walls of several houses were blown away, a small pick-up truck flipped over and it ended up against a palm tree and a large camper was pushed backwards about 30*m* and pinned against a row of palm trees. The beach area here is backed by marshy wetlands. The wave penetrated up the river and into the marsh and overturned boats were observed over 500*m* inland. No one was killed in Boca de Iguanas but several houses were entirely destroyed by the wave. Runup in Boca de Iguanas was measured in several different locations and varied

between 3.5 and 5*m*. An offshore tsunami record—an important and rare set of data—was also generated by this tsunami.Two moorings of bottom mounted pressure sensors had just been installed offshore of La Manzanilla for a study of internal wave motions. The sensors were installed by Filonov, A.E. and other scientists from the University of Guadalajara just one week before the tsunami struck. This array of sensors recorded a tsunami train propagating to shore, offshore at about 50*m* water depth (Filonov, 1997).

4.6.3 Numerical model

This event was remarkable due to the unique data set obtained both about tsunami waves and about the co-seismic displacement of the earthquake source. The focus of the numerical simulation of this tsunami was an attempt to construct a numerical model of this event consistent with both seismic data and bottom pressure sensors data sets. The numerical modeling of this event was performed using the VTCS-3 model and included the runup computations. The digital bathymetry[1] used for the computation covers more then 300*km* of the affected Mexican coastline. It consists of three levels of nested grids with different resolutions as shown on Figure 4.55. The largest array A is interpolated from the TOPO5 digital bathymetry and has grid resolution of 1350*m*; the array B has smaller grid spacing of 450*m* and is interpolated from A, the two smallest arrays C and D are digitized from the nautical charts and topographical maps, and they have resolution of 150*m*.

1. Modesto Ortiz from the Centro de Investigacion Cientifica, Desarollo Tecnologico y de Educacion Superior (CICESE) of Ensanada, Mexico helped to generate the digital data.

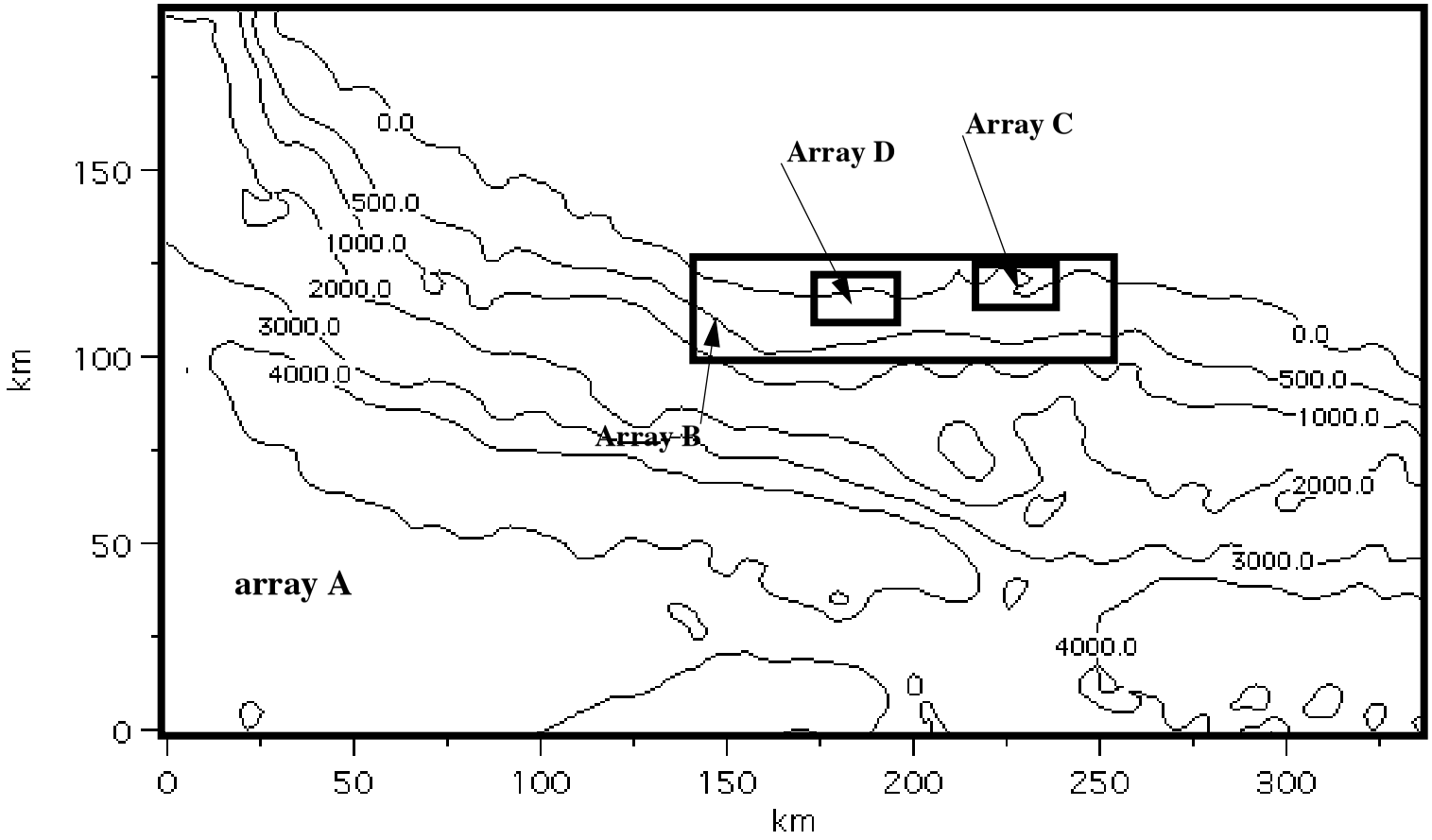

Figure 4.55 The computational grid arrangement for the Mexican tsunami modeling.

The model tsunami source was designed to agree with the GPS displacement data of Melbourne et. al. (1996). The inversion of the data shows two distinct slip patches on the fault plane suggesting two-fault source (Melbourne et. al., 1996). Hence, the tsunami source was constructed as a two-fault model. The orientations of each of the fault planes were taken similar to the Harvard CMT estimation with dip = 16˚, strike = 309˚ and slip = 90˚. The dimensions and slip amount of the faults were inferred from the slip distribution obtained by Melbourne et al. (1996). Eleven trial computation were conducted changing slightly the positions of the fault planes and their average slip values. The fault parameters of the South (S) and North (N) planes used for these computations are shown in Table 3.

Table 3 THE FAULT PARAMETERS OF THE TRIAL COMPUTATIONS

No	X-coordinate of low-left corner (grid points)	Y-coordinate of low-left corner (grid points)	Slip amount $U_0(m)$	Fault length L(*km*)	Fault width W(*km*)
1 S	206	68	3	80	35
N	136	55	4	80	30
1 S	200	51	2	70	50
N	135	44	4	100	40
3 S	198	55	2	70	45
N	135	37	4	100	50
4 S	198	55	2	70	45
N	135	37	4	100	50
5 S	198	65	2	70	45
N	135	42	4	100	50
6 S	198	65	2	70	45
N	135	35	3.5	100	60

Table 3 THE FAULT PARAMETERS OF THE TRIAL COMPUTATIONS

No	X-coordinate of low-left corner (grid points)	Y-coordinate of low-left corner (grid points)	Slip amount $U_0(m)$	Fault length L(*km*)	Fault width W(*km*)
7 S N	198 135	65 30	2 3.5	70 100	45 60
8 S N	198 135	65 30	2 3	70 100	45 60
9 S **N**	**198** **135**	**65** **37**	**2** **3**	**70** **100**	**45** **50**
10 S N	190 135	70 37	2 3	60 100	40 50

The results of the computed tsunami wave were compared with the offshore gage record of Filonov (1997). The source number 9 shown on Figure 4.56 demonstrated the best fit with the data. Figure 4.57 shows the comparison of the computed and measured tsunami records for this source.

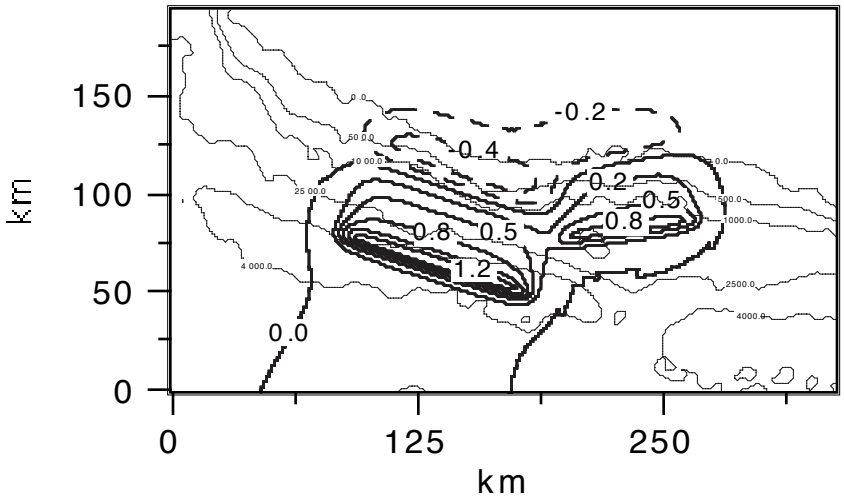

Figure 4.56 Contours of the sea floor deformation of the tsunami source 9 from Table 3.

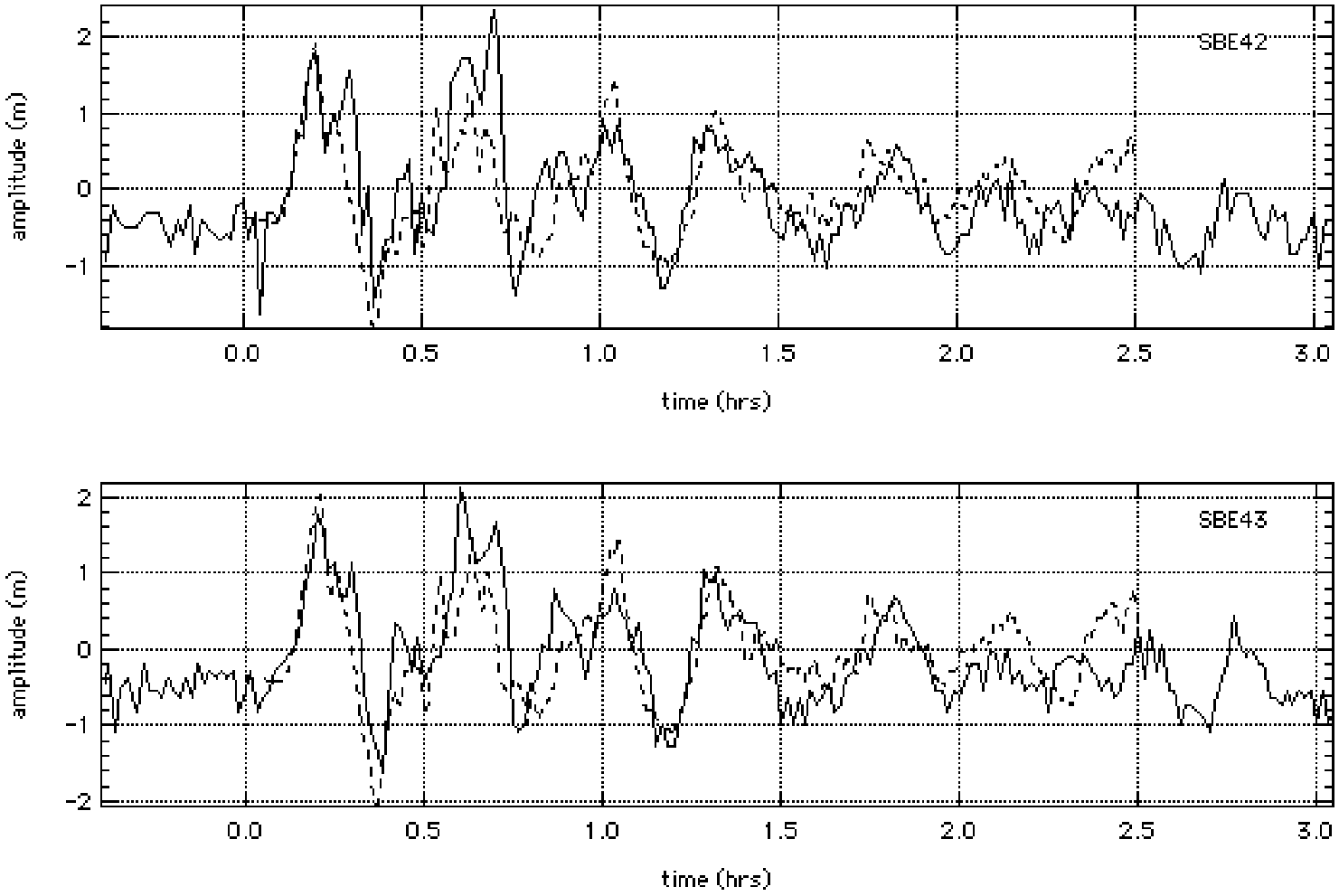

Figure 4.57 Comparison between the computed (dashed) and measured (solid) tsunami profiles.

The area where the instruments were located has subsided after the earthquake by approximately 35*cm* and a new water level was established. The plot on Figure 4.57 has this new sea level as zero *y*-coordinate. The distance between the two instruments (SBE42 and SBE43) is only 240*m*, consequently the recorded signals are very similar. The comparison shows that not only the first (incoming) wave was modeled correctly, but also several consequent oscillations of the computed wave, which include multiple reflection from the shore and trapped waves, they all are very close to the measurements. This demonstrate that the source dimensions, which determine the tsunami wavelength, and its position were anticipated correctly in the source 9, at least for the closest fault plane.

4.7 Summary and conclusions

In this chapter the numerical model was applied to simulate several historic tsunamis. Both described models, 1+1 and 2+1 approximations, were used for the calculations. These numerical experiments show that the numerical algorithm described in chapters 2 and 3 is capable of simulating realistic events. The numerical model reproduces important characteristics of tsunami waves, such as runup heights, inundation boundaries and flow velocities quantitatively and qualitatively similar to observations.